Dear author,

Please note that changes made in the online proofing system will be added to the article before publication but are not reflected in this PDF.

We also ask that this file not be used for submitting corrections.

food and bioproducts processing xxx (2016) xxx–xxx

Contents lists available at ScienceDirect

Food and Bioproducts Processing

journal homepage: www.elsevier.com/locate/fbp

Determining the optimal shaking rate of a reciprocal agitation sterilization system for liquid foods: A computational approach with experimental validation

Ferruh Erdogdu[a,*], *Mustafa Tutar*[b,c], *Sigurd Oines*[d], *Igor Barreno*[e], *Dagbjorn Skipnes*[d]

[a] *Department of Food Engineering, Ankara University, Ankara, Turkey*
[b] *Mechanical and Manufacturing Department, MGEP Mondragon Goi Eskola Politeknikoa, Spain*
[c] *IKERBASQUE, Basque Foundation for Science, Spain*
[d] *Department of Process Technology, Nofima, AS, Norway*
[e] *CS Centro Stirling S. Coop, Aretxabaleta, Spain*

ARTICLE INFO

Article history:
Received 22 February 2016
Received in revised form 19 July 2016
Accepted 22 July 2016
Available online xxx

Keywords:
Canned foods
Optimization
Modelling
Reciprocal agitation - shaking

ABSTRACT

A new canning process where a reciprocating agitation is carried out in horizontally oriented containers has been recently demonstrated to reduce processing times and enable energy savings with less degradation in the quality of processed food products. Reciprocal agitation by imposing additional forces enhances convective mixing with increased production efficiency. The reciprocal agitation uses the horizontal acceleration in addition to gravity and sum of these forces lead to a considerable increase in the heat transfer rates. In the literature, there have been experimental approaches to evaluate heat transfer enhancement. However, due to the balance among these forces, there might be an optimum reciprocal agitation rate for the increased heat transfer depending upon the physical properties of the liquid processed. Therefore, the objectives of this study were to determine the optimum agitation rates by developing a computational model for heat transfer. For this purpose, a multi-phase model simulation was performed using a finite volume method based on discretization of governing flow equations for liquid and gas phase in a non-inertial reference frame of moving mesh. Experimental studies for model validation were carried out in a reciprocally agitated retort using 98.2 mm × 115 mm cans containing distilled water with 2% headspace as a model case. The model results were in agreement with the experimental data, and the optimum reciprocal agitation rate was determined. The results of this study are to be used to optimize the process with respect to improve the health-promoting compounds of processed foods.

1. Introduction

Traditional canning has been a convenient way and provided a generalist and economic method for processing and preservation of food products. Consumer demands for high quality foods, however, force the food processors to improve and innovate their processing. It is a well-known fact that the shorter the process time at a given process condition, while still achieving the required safety for consumption, the less the damage to the sensory and nutritive quality of the food products. Based on this concept, following the use

* Corresponding author. Tel.: +90 533 812 0686; fax: +90 312 317 8711.
E-mail addresses: ferruherdogdu@ankara.edu.tr, ferruherdogdu@yahoo.com (F. Erdogdu).
http://dx.doi.org/10.1016/j.fbp.2016.07.012

of retorts for canning, the agitation retorts were introduced in 1920s with the agitation mechanism based on horizontal axial rotation (Ates et al., 2014). Vertical rotation of the cans was later introduced with the end-over-end rotation principle (Clifcorn et al., 1950). Introduction of agitation mechanism in canning for liquid or liquid–solid particles containing food products was the result of a certain disadvantage of the static retort systems (Rosnes et al., 2011). The primary challenge in the static processing is the slow heat penetration resulting in a lack of consistency in sensory and nutritive properties (Ohlsson, 1980).

Considering the effective heat transfer rates obtained with agitation, a reciprocating horizontal agitation with rapid back and forth motion of the horizontal containers in an oscillating way has been proposed to increase the heat transfer rate further, and an agitating retort with high frequency longitudinal mechanism was developed in 2006 (Ates et al., 2014). Both horizontal and end-over-end based agitation retorts suffer from the limitation of that the applied forces to enable the motion within the container were a balance between gravity and centrifugal forces (Walden and Emanuel, 2010). Due to this balance, the agitation increases the heat transfer rate up to an optimum while further agitation might not affect or might influence the process in a negative way depending especially upon the viscosity of food product. A detailed analysis and comparison among the gravity and centrifugal forces for the case of axial rotation effects in horizontal axial rotation of cans were reported by Erdogdu and Tutar (2012) and Tutar and Erdogdu (2012). The reciprocal agitation, however, used the horizontal acceleration in addition to gravity, and the sum of these forces enabled a considerable increase in the heat transfer rates with reductions in the process time (Walden and Emanuel, 2010).

The first studies in the food engineering literature using the reciprocating agitation systems were experimental based to demonstrate the possible process time reductions and improvements in the heat transfer rates. Bermudez-Aguirre et al. (2013a) demonstrated the improvement in heat transfer coefficient under static and horizontal gentle-rocking modes. Ates et al. (2014), for example, compared the novel agitating retort and static retort processes for bacterial inactivation, and it was concluded that agitating retort process significantly lowered the required process time. The study by Singh et al. (2015a) focused on evaluating the heat transfer enhancement under reciprocal agitation while Singh et al. (2015b) developed an experimental methodology to determine the heat transfer coefficient in canned particulate fluids under reciprocating frequencies up to 3 Hz. Singh and Ramaswamy (2015a) focused on the effect of product related parameters on heat transfer while Singh and Ramaswamy (2015b) determined the effect of the orientation of cans during reciprocating agitation thermal processing. Singh et al. (2016) introduced the concept of reciprocal agitation process to improve the quality of canned green beans during thermal processing. Singh and Ramaswamy (2016) carried out an optimization study for the heat transfer rate and reciprocation intensity for thermal processing of liquid particulate mixtures. These studies were based on experimental approaches while a similar situation was explored by Liffman et al. (1997) and Pesch et al. (2008) in a computational–theoretical way for convection due to horizontal shaking and heated fluid layers subjected to time-periodic horizontal accelerations, respectively.

Even though there were certain findings reported for the effect of reciprocal agitation on the temperature increase and enhanced heat transfer rate (Bermudez-Aguirre et al., 2013a; Ates et al., 2014; Singh and Ramaswamy, 2015a,b, 2016; Singh et al., 2016), development of a computational model (with one exception where the heat transfer coefficient based lumped model without considering the temperature distribution was introduced by Bermudez-Aguirre et al. (2013b) and determining the optimal agitation rates were not focused in detail. For determining the optimal conditions, one exception was reported by Singh and Ramaswamy (2016) where the optimal conditions of reciprocation intensity for liquid particulate mixtures were experimentally determined. The optimization studies based on a computational model are significant since the computational model might also be used also for process development purposes. Therefore, the primary objective of this study was to determine the optimal agitation rate in a reciprocal agitation process using an experimentally validated computational model. The secondary objectives were first to develop a computational numerical model for heat and momentum transfer inside the reciprocally agitated cans to determine the temperature distribution and velocity changes and then experimentally validate the model.

2. Materials and methods

For the given objectives, the study consisted of experimental and computational parts. In the experimental part, a water filled can was processed in boiling water and agitating conditions. In both cases, the horizontally oriented can contained water as a test liquid to represent a low viscosity Newtonian liquid. The time–temperature data obtained at the geometric center in the first experiments were used to develop and validate the computational model, to decide upon the computational parameters with the mesh independency studies. Following the mesh independency study, the computational model was validated with the temperature data obtained under horizontal agitating conditions, and the model was applied to horizontal agitation rates from 20 to 140 rpm to obtain the agitation rate in the direction of the axis of the horizontal can resulting in maximum heat transfer. In the reciprocal agitation systems, the crankshaft, used to derive the horizontal motion, angular velocity is related to engine revolutions per min (rpm).

2.1. *Experimental methodology*

The first step in this study was to decide upon the computational parameters and test the accuracy of the computational method. For this objective, an experimental study with a canned water sample (98.2 mm × 115 mm cans filled with distilled water with 2% headspace) was carried out in a Microflow 911 EAT Shaka retort (Steriflow, Roanne, France) in boiling water under stationary conditions. The retort system was heated by direct steam injection, equipped with a preheating tank to process water. This processed water was then circulated through a heat exchanger (only used for cooling) to the retort and spread by a perforated plate to obtain water raining over the cans. The can was fixed in a horizontal position in the boiling water. Type-T thermocouple connected to a data logger E-Val Flez (Ellab, Copenhagen, Denmark) was located at the geometrical center using ring gaskets and locking-receptacles. The experimental set-up was shown in Fig. 1.

The can material was a steel sheet with a thickness of 0.19 mm and thermal conductivity value of 15–16 W/m^2 K. This enabled the assumption of the negligible conduction effect of

Please cite this article in press as: Erdogdu, F., et al., Determining the optimal shaking rate of a reciprocal agitation sterilization system for liquid foods: A computational approach with experimental validation. Food Bioprod Process (2016), http://dx.doi.org/10.1016/j.fbp.2016.07.012

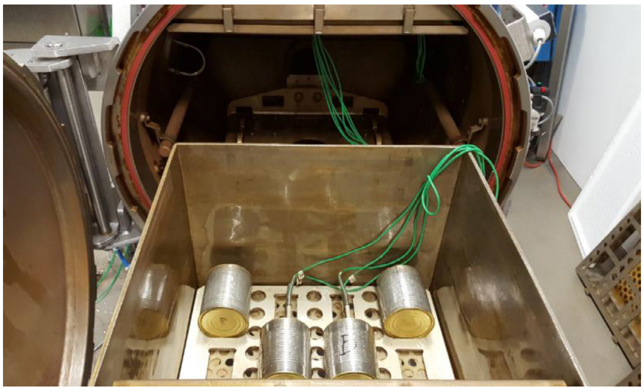

Fig. 1 – Experimental set-up where the can was fixed in a horizontal position with installed type-T thermocouples.

can wall on the heat transfer, and the medium temperature was accepted to be the can surface temperature.

In the second group of the experiments, the same can was used under horizontally agitation conditions where the shaking rate changed from 0 rpm (in the first 26 s of the process) to 80 rpm (at the 35 s of the process). Since the horizontal-accelerated agitation rates were included in this model validation part of the study, the agitation rates were first converted to the tangential velocity values. For this purpose, since a horizontal agitated system used a slider – crank derived mechanism (Fig. 2a – modified from Reader and Hooper, 1982), displacement of the can during the agitation process was defined with the following equation:

$$x_p = \left[r - r \cdot (1 - \sin(\omega \cdot t)) + n \cdot \left(1 - \left(1 - \frac{\cos^2(\omega \cdot t)}{n^2} \right)^{0.5} \right) \right] \quad (1)$$

where $n = L/r$, x is the displacement (m), ω is the shaking rate (rpm), t is the time (s), r is the crank radius of the system (0.075 m), and L is the length of the connectivity rod (0.5 m). Since ($n^2 >> \cos^2(\omega \cdot t)$), this equation was then simplified with:

$$x_p = [r \cdot \sin(\omega \cdot t)] \quad (2)$$

The comparison of Eqs. (1) and (2) for the change of displacement with respect to the ($\omega \cdot t$) values did not show any significant difference resulting in very same displacement values. Therefore, the second equation with its simplified form

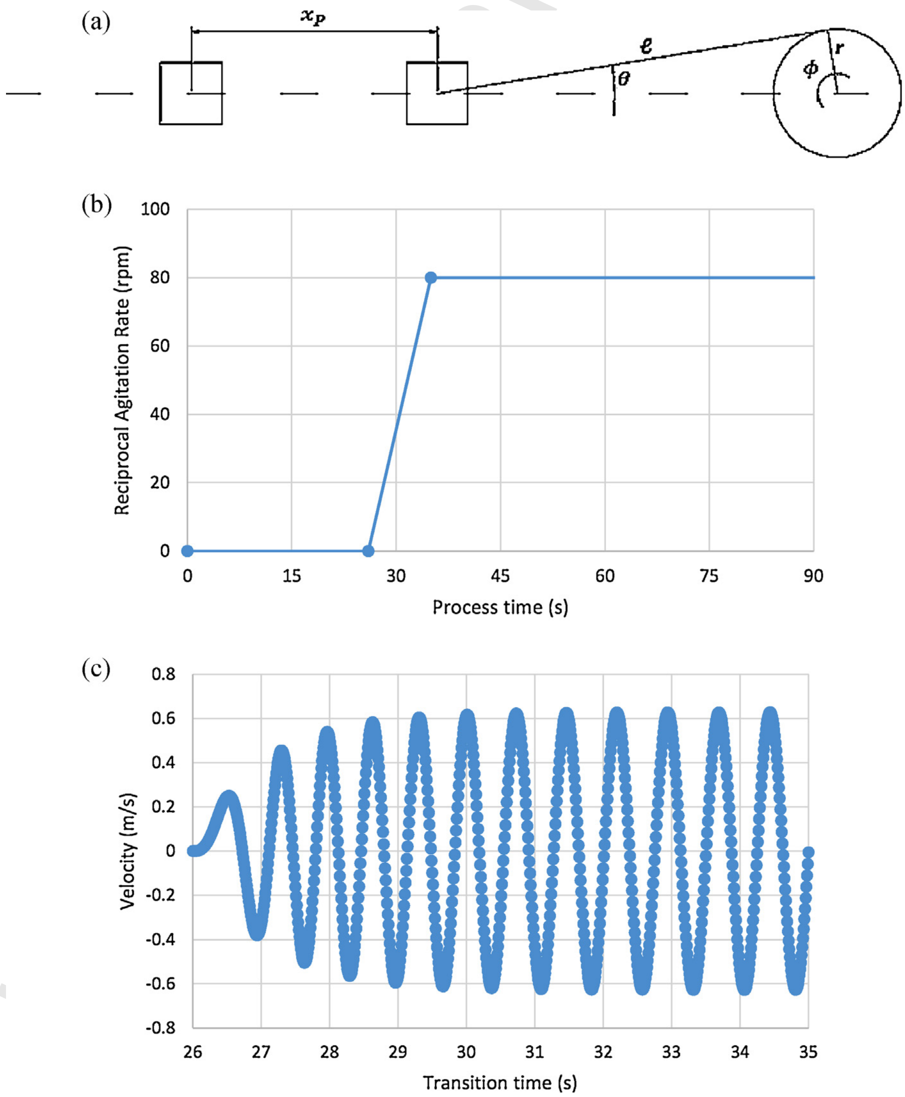

Fig. 2 – (a) A horizontal agitated system with a slider – crank derived mechanism (modified from Reader and Hooper, 1982); (b) reciprocal agitation rate used in the second set of model validation experiments; (c) tangential velocity change in the transition perid from 0 ro 80 rpm reciprocal agitation rate.

was chosen to derive the tangential velocity equation for the reciprocal agitation system:

$$v = r \cdot \omega \cdot \cos\ (\omega \cdot t) \tag{3}$$

However, this equation brought the issue of non-zero velocity at the beginning of the horizontal agitation process. This resulted in the instabilities and non-convergence problems in the numerical computations. To prevent this and to make sure that the process start with a '0' velocity initially, the movement was displaced with one period, and the following velocity equation was preferred to start with:

$$\begin{aligned} &v = r \cdot \omega \cdot \sin\ (\omega \cdot t) \\ &\lim_{t \to 0} v = 0 \end{aligned} \tag{4}$$

As explained in the experimental set-up for model validation, following the initial steady 26 s, reciprocal agitation transition of the system was from 0 to a higher agitation rate of 80 rpm [0.623 m/s]. This transition period took 9 s and was assumed to follow an exponential increase. The exponential increase from 0 velocity to 80 rpm reciprocal agitation rate was preferred to enable the smooth transition between these rates. The exponential increase was the only way for this smooth transition and to prevent the overshoot after 9 s of the transition period. Among various trials, the linear increase for example resulted in a sharp transition to the 80 rpm, which might be rather difficult to control physically. To conform the transition period with 80 rpm of reciprocal agitation rate after 9 s smoothly, the given values below for the following transition stage equation, where the velocity change in the transition period was shown, enabled this:

$$v = \frac{80[\text{rpm}]}{60[\text{s/min}]} \cdot [1 - \exp(-k \cdot t')] \tag{5}$$

where ($k = 1$) is the constant (s^{-1}) and $t' = (t - 26)$ (s). Fig. 2b shows the horizontal agitation rate through the experiments while Fig. 2c demonstrate the velocity profile from 0 to 80 rpm in the transition period of 9 s (from 26 to 35 s). The change in the horizontal agitation rate, as reported in Fig. 2b, c, and the variable – experimentally recorded medium temperature were used in the model validation case to compare the numerical results with the experimental one obtained at the centre of the can.

For both cases, 3-experiments were carried out, the average values with the standard deviation were used in the model validation. Since the standard deviations of the average of the temperature change based on these three experiments, additional experiments were avoided.

2.2. *Governing equations and the computational model*

The numerical methodology and full scale model experimental testing verifications proposed a useful computational algorithm for dynamic monitoring of headspace (air) and liquid (water) interactions through the agitation and solved the fluid-thermal energy interactions in order to optimize the reciprocal agitation process. The two-phase volume of fluid (VOF) approach accompanied with the finite volume method (FVM) based numerical discretization scheme was utilized in the simulation of two-phase flow under varying physical conditions through unsteady, three-dimensional and turbulent flow simulations for the given Rayleigh number range over 1E9 at the initial phase of the heating as explained below.

The basic mathematical model for the discretization process included the solution of fundamental governing equations of fluid flow motion, known as continuity equation and momentum conservation equations, i.e., Navier-Stokes (N-S) equations for incompressible fluid in a non-inertial frame:

2.3. *Continuity equation*

$$\frac{\partial \rho}{\partial t} + \nabla \rho \vec{v}_r = 0 \tag{6}$$

2.4. *Momentum equation*

$$\frac{\partial}{\partial t}(\rho \vec{v}_r) + \nabla(\rho \vec{v}_r \vec{v}_r) = -\nabla P + \nabla \bar{\bar{\tau}}_r + \vec{F} \tag{7}$$

where ρ was the density (kg m^{-3}), t was the time (s), $\vec{v}_r$ was the relative velocity vector of a fluid particle (m s^{-1}), P was the static pressure (Pa), $\bar{\bar{\tau}}_r$ was the stress tensor (described below), $\vec{F}$ was the external body force (N) including gravitational effects and acceleration due to the non-inertial frame motion. The stress tensor, $\bar{\bar{\tau}}_r$ was:

$$\bar{\bar{\tau}} = \mu[(\nabla \vec{v}_r + \nabla \vec{v}_r^T) - \frac{2}{3} \nabla \vec{v}_r I] \tag{8}$$

where μ was the dynamic viscosity (Pa s). It was defined to be a temperature dependent polynomial function. I was the unit tensor, and the second term on the right hand side was the effect of volume dilation. The volume dilation was neglected in the solutions since there was no effect in the process. Energy conservation equation, also solved for the present flow, was written in terms of relative internal energy (E_r) and relative total enthalpy (H_r):

2.5. *Energy equation*

$$\frac{\partial}{\partial t} \rho E_r + \nabla(\rho \vec{v}_r H_r) = \nabla(k \nabla T + \bar{\bar{\tau}}_r) + S_h \tag{9}$$

where

$$E_r = h - \frac{P}{\rho} + \frac{1}{2}(v_r^2 - u_r^2) \tag{10}$$

$$H_r = E_r + \frac{P}{\rho} \tag{11}$$

Velocity evolutions were then transformed from stationary to rotating frame using:

$$\vec{v}_r = \vec{v} - \vec{u}_r \tag{12}$$

where $\vec{v}_r$ was the relative velocity (m s^{-1}) arising from the mesh motion (velocity viewed from the moving mesh of the oscillatory reciprocating motion), $\vec{v}$ was the absolute velocity (m s^{-1}) (velocity viewed from the stationary frame), and $\vec{u}_r$ was the longitudinal velocity (m s^{-1}) (velocity due to the moving mesh). The above governing equations were directly discretized with a finite volume method (FVM) in conjunction with an interface tracking model (as described below) for the air–liquid system. Reynolds-averaged Navier-Stokes (RANS) based form of these equations were discretized together with the transport equations of turbulence kinetic energy and its dissipation within the finite volume scheme by using the RANS

Please cite this article in press as: Erdogdu, F., et al., Determining the optimal shaking rate of a reciprocal agitation sterilization system for liquid foods: A computational approach with experimental validation. Food Bioprod Process (2016), http://dx.doi.org/10.1016/j.fbp.2016.07.012

based k-ε turbulence closure model (Yakhot and Orszag, 1986) accompanied with the utilized interface tracking model at higher agitation rates.

Julien et al. (1996) reported the ‘soft’ and ‘hard’ turbulence conditions led by the higher Rayleigh numbers, and the lower ranges where the Rayleigh number (Ra) was smaller than 1E7, was characterized by soft turbulence conditions by Kooij et al. (2015). The initial Rayleigh number for the first experimental case was 2.66E9 (this value was obtained at the 0.5 s of the model validation simulation where there was no movement of the can) where it was beyond the soft turbulence case. Even though the Rayleigh number, as a product of Grashof and Prandtl number, determined the turbulence inducement in the natural convection flow in the cylindrical cavity, local cell Reynolds (Re_L) number change was also controlled. It was up to 30 along the surface of the can at the initial phase of the stationary model validation case (0.5 s) while it increased up to 100 towards the end. The turbulence Reynolds number (Re_T) was, on the other hand, high enough to resolve the present flow with a turbulence model, with its instantaneous local value up to 18,400 initially at the centre of the horizontal cylindrical cavity. The Rayleigh and local Reynolds and turbulence Reynolds number were determined using Eq. (13):

$$\begin{aligned} Ra &= \frac{g\cdot\beta\cdot\Delta T\cdot D^3}{(\mu/\rho)^2}\cdot Pr \\ Re_L &= \frac{V_c{}^{1/3}\cdot \upsilon\cdot\rho}{\mu} \\ Re_T &= \frac{k^2\cdot\rho}{\mu\cdot\varepsilon} \end{aligned} \tag{13}$$

where g was the gravitational acceleration (m/s^2), β was thermal expansion coefficient for water (1/K), ΔT was the maximum temperature difference between the heating medium and the initial temperature of the system (K), D was the characteristic dimension (diameter of the cylindrical cavity, m), Pr was Prandtl number, and μ was the dynamic viscosity (Pa s), ρ was the density (kg/m^3), ν was the velocity encountered in a given cell (m/s), and $V_c^{1/3}$ was the characteristic length of the local cell, and $k\varepsilon$ were turbulence kinetic energy and dissipation rate, respectively. Besides high Rayleigh number encountered at the initial phase of the process, the laminar flow condition was still tested for convergence during the initial test simulations, but these trials resulted in convergence problems. Therefore, based on the Rayleigh number information for turbulence conditions and considering the results of the initial simulations for model validation purposes, the turbulence model was activated in the simulations. In addition, for the simulation study carried out under steady conditions for model validation – mesh independency study, the turbulence Reynolds number was around 80 toward the end of the simulation.

For the turbulence model, the following turbulence parameters were applied:

- Initial turbulence intensity (I) was assumed to be 5%, Based on the maximum tangential velocity value of 1.1 m/s (obtained by Eq. (4)), the turbulence kinetic energy value (k) was 0.00453 m^2/s^2:

$$k = \frac{3}{2}\cdot(\upsilon_{\max}\cdot I)^2 = 0.00453 \tag{14}$$

- Turbulence dissipation rate (ε) was 0.025 m^2/a:

$$\varepsilon = C_\mu^{3/4}\cdot\frac{k^{3/2}}{L} = 0.025 \tag{15}$$

where L was the turbulent length scale (0.002 m), and C_μ was turbulence model constant (0.09).

The tracking of interface between air–water phases was accomplished through the volume of fluid (VOF) method proposed by Hirt and Nichols (1981). In this model, a single set of momentum equations was shared by the fluids and the volume fractions of each of the fluids in each computational cell were tracked through the domain. The fields for all variables and properties are shared by phases and represents volume-averaged values as long as the volume fraction of each of the phases is known at each location. Thus, the variables and properties in any given cell are either purely representative of one of the phases or representative of mixture of phases depending on the volume fraction values. The volume fractions of water and air in the computational cell sum to unity. Interface tracking was carried out by solving continuity equation for volume fraction of one of the phases where air was specified as primary phase and thus the volume fraction of the liquid phase was solved. In addition to VOF method, Ubbink’s compressive interface capturing scheme (Ubbink and Issaa, 1999) for arbitrary meshes (CICSAM) was also applied.

For the numerical solution procedure, a finite volume method (FVM) based solver (Ansys Fluent V15, Ansys, Inc., Canonsburg, PA, USA) was used to solve the preceding partial differential governing equations of the present two-phase flow problem. In the proposed computational model, the collocated FVM was employed to discretize the governing 3D flow-energy equations. All the required thermal and physical properties for air and water phases were temperature dependent and reported in Erdogdu and Tutar (2012). Initially, water in the can in both experimental condition was at rest and had the initial temperature of 300.92 and 301.38 K in the steady and agitation cases, respectively. While the boiling water temperature and variable medium temperatures were used in the model validation simulation, a uniform constant wall temperature of (T_w = 373.15 K) was used to determine the effect of reciprocal agitation rates on the temperature evolution. For the case of agitation process, the heating medium temperature was variable, but it was still used to be as a constant wall temperature over the can surface due to the rapid movement of the can during the process. Over the initial period of the agitation process where there was no reciprocal movement of the can (Fig. 2c), the heating medium temperature and the initial temperature of the can were similar. Therefore, the given assumption was assumed to hold true during the initial period. The surface tension value along the interface of air and water was assigned to be 0.72 N/m, and the time step size used in all simulations was 1E−4 s.

3. Results and discussion

3.1. Model validation

Using the results of the first experimental data set, the simulation schemes were decided:

- a pressure based solver with the absolute velocity formulation,

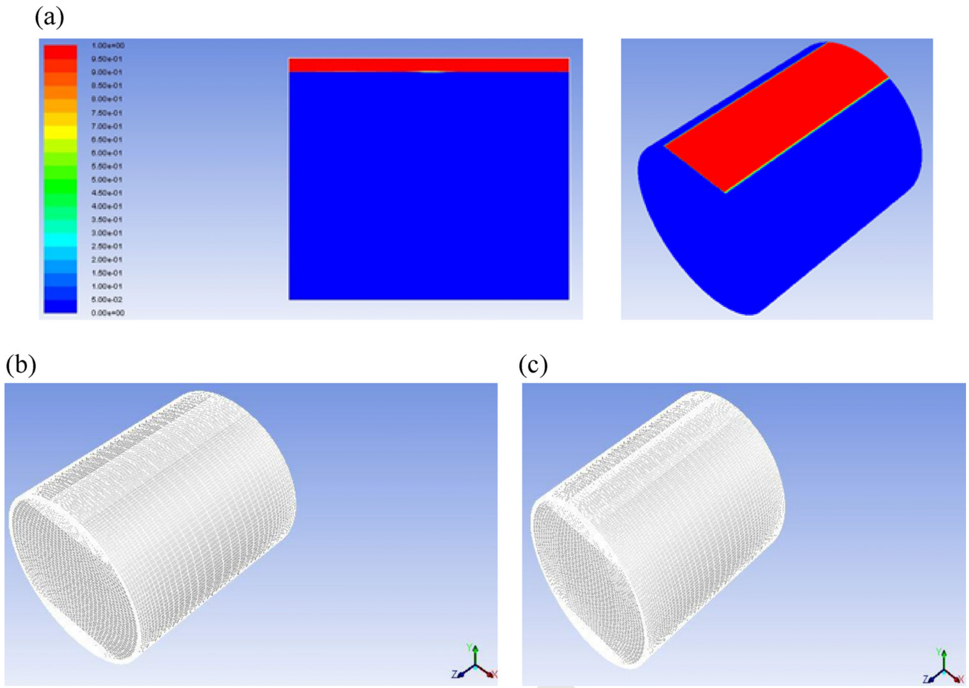

Fig. 3 – Initial phase contours of the geometry with air (at the top) and water phases (a) and the mesh structures adopted for (b) the minimum – 199,728 and (c) the maximum – 337,800 sized meshes.

- the pressure-velocity coupling was carried out with PISO (pressure implicit with splitting of operator) scheme with skewness-neighbour coupling,
- transient formulation was first order implicit, and
- spatial discretization for gradient was Green-Gauss node based; for pressure PRESTO; for momentum first order upwind; for volume fraction CICSAM; and for turbulence kinetic energy first order upwind schemes were used. Even though the first order upwind scheme is too dissipative to stabilize the computation, the initial simulation studies confirmed that the given solution schemers suit better for straight convergence and stabilized computation for the chosen time step size and mesh resolution. Besides, regarding the order of the discretization scheme, the system uncertainty as well as the turbulence model uncertainty might be larger than the error caused by numerical dissipation.

Using these schemes, the computational model was first applied to study mesh independency and hence to determine the final mesh configuration based on the first set of experimental results. Then, the model validation study was carried out under a reciprocal agitation condition, and the reciprocally agitating speeds from 20 to 140 rpm were then tested for temperature change during the agitation to determine the effect of agitation and optimum agitation rate.

Fig. 3 shows the initial phase contours of the geometry with head space – air (at the top) and water phases and the mesh structures adopted for the minimum (199,728 cells) and maximum (337,800 cells) numbered mesh configurations. Fig. 4a shows the results of mesh independency study with respect to experimental data obtained at the centre of the horizontal can located in boiling water. There was not a significant difference between the 199,728 and 286,080 cells while the 337,800 cell structured mesh over-predicted the temperature (Fig. 4a). This difference might be due to the context of mesh-density – round-off error relation. Though round-off errors may be accumulated more with higher number of mesh cells, further round-off analysis might be required to identify their effect on the mesh structure and resolution for different time-step sizes. However, it should be emphasized that the flow system uncertainty as well as the turbulence model uncertainty for

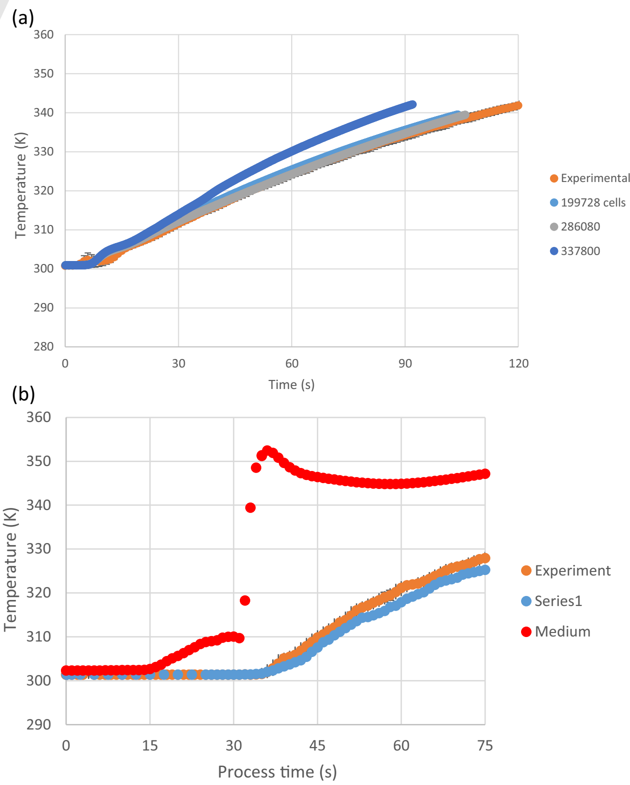

Fig. 4 – Comparison of experimental data with the simulation results (a) experimental data obtained at the centre of a horizontally placed static can in boiling water with; (b) experimental data obtained at the centre of a horizontally placed static can under reciprocally agitating conditions (the mesh structure used in both computational models had 199,728 cells).

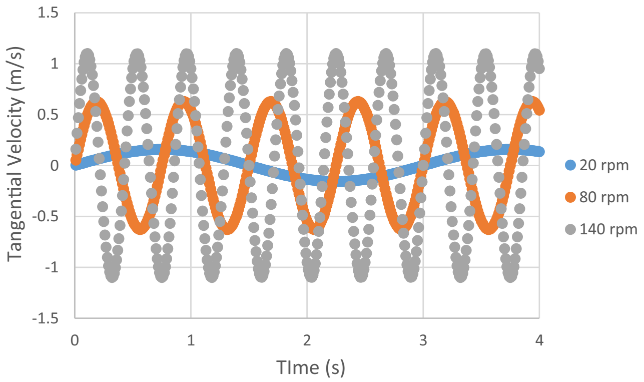

Fig. 5 – Comparison of tangential velocity change versus reciprocal agitation rates.

the choice of mesh resolution and time step size accompanied could be significant on the flow results in addition to the order of the spatial discretization scheme and relaxation parameters. There could/may be no straightforward solution for minimum numerical diffusion and higher accuracy with use of very high mesh resolution accompanied with smaller time step size and higher order spatial discretization scheme. The mesh independency simulations and the initial simulations have demonstrate that the selected time step size of 1E−4 s for the generated mesh resolution of 199,728 mesh cells were accurate enough to obtain results which would be in good correspondence with the experimental data. Therefore, based on the mesh independency results, the mesh structure with 199,728 cells was used in the second part of the model

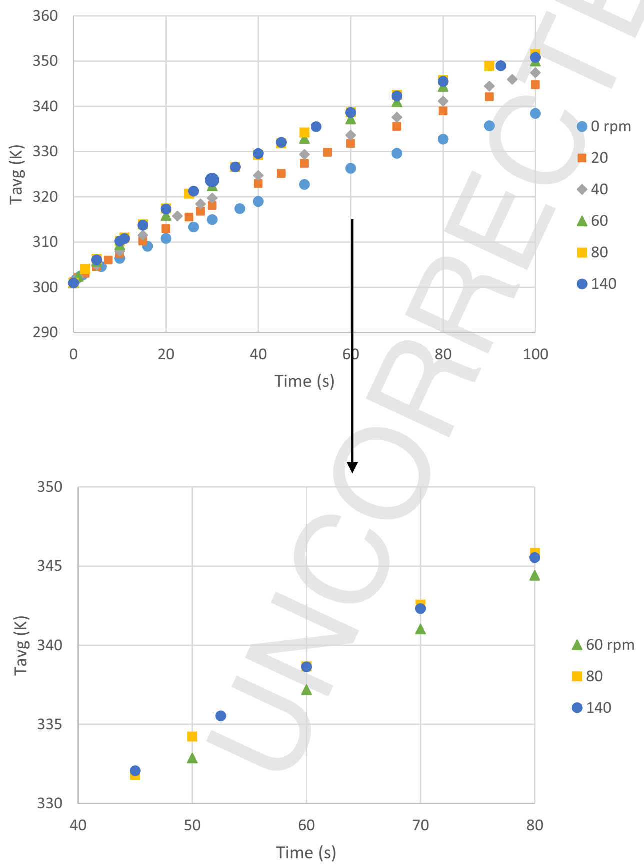

Fig. 6 – Effect of reciprocal agitation rate on the volume average increase of temperature.

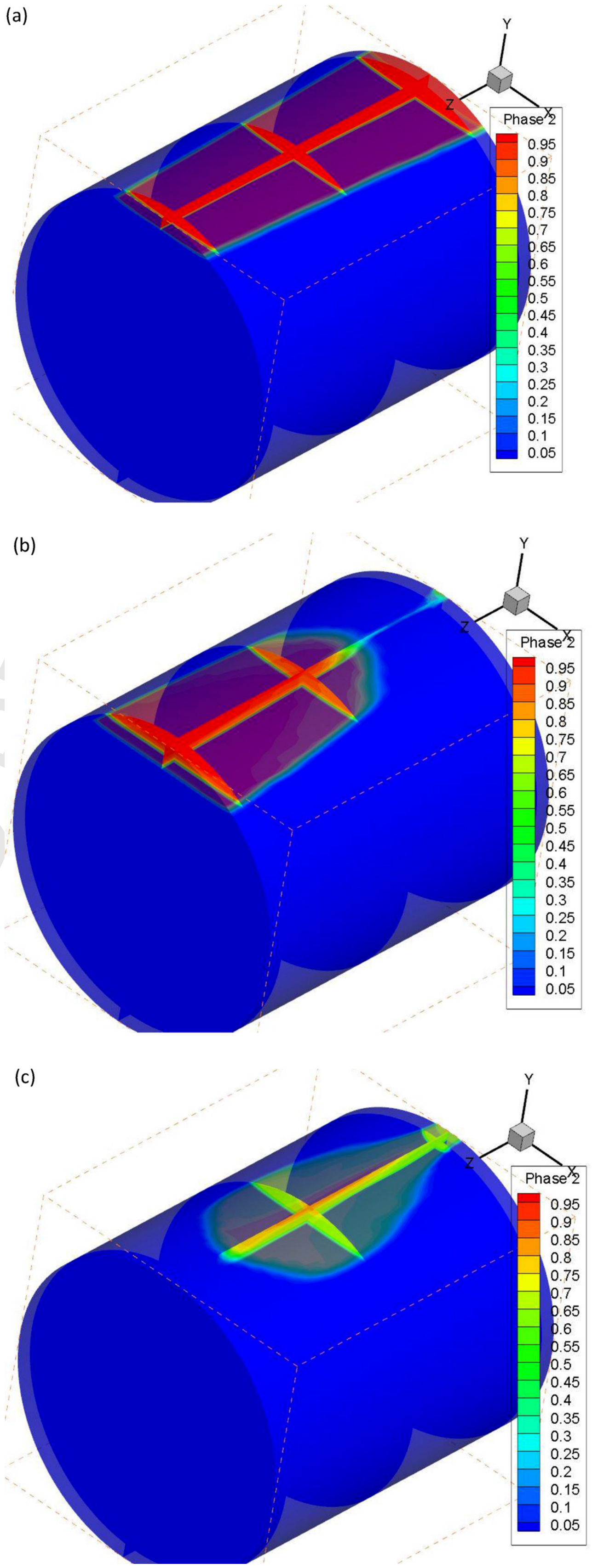

Fig. 7 – Phase contours in the various x- and z-planes of the computational geometry at the (a) beginning (1 s); (b) 30 s; and (c) 90 s of the 20 rpm reciprocal agitation case.

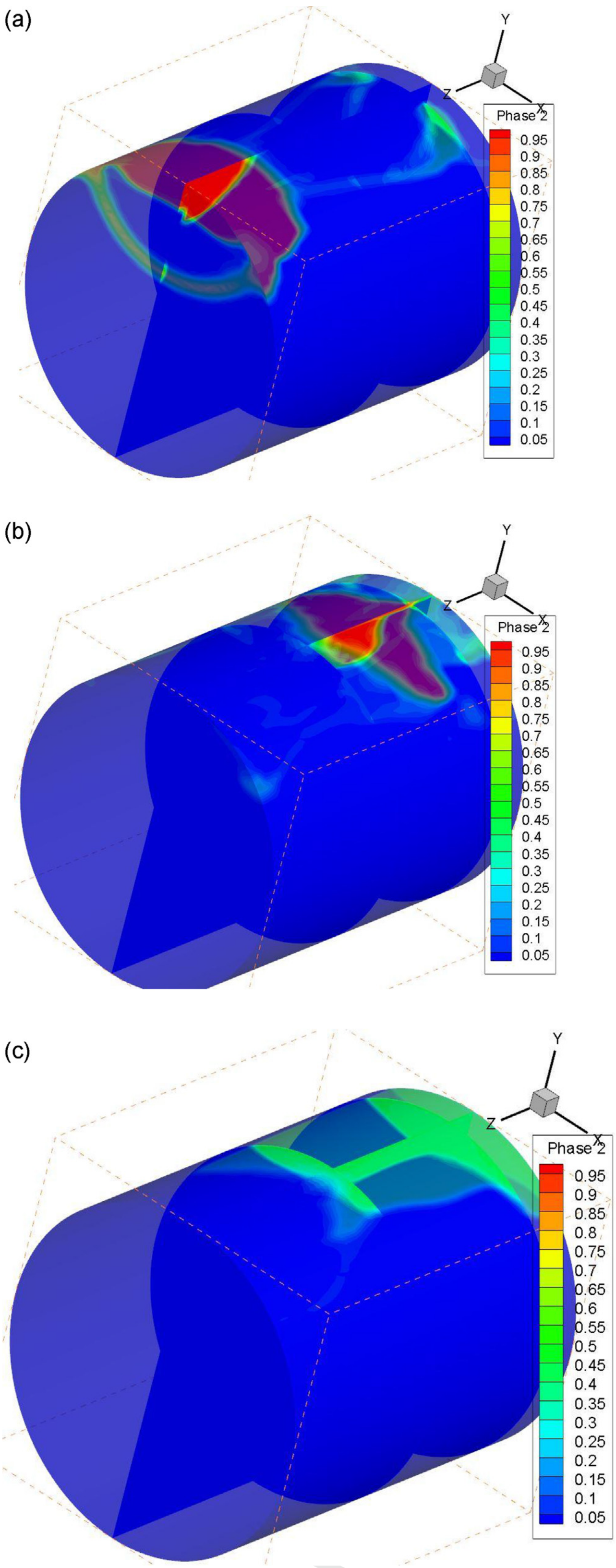

Fig. 8 – Phase contours in the various *x*- and z-planes of the computational geometry at the (a) beginning (1 s); (b) 30 s; and (c) 90 s of the 80 rpm reciprocal agitation case.

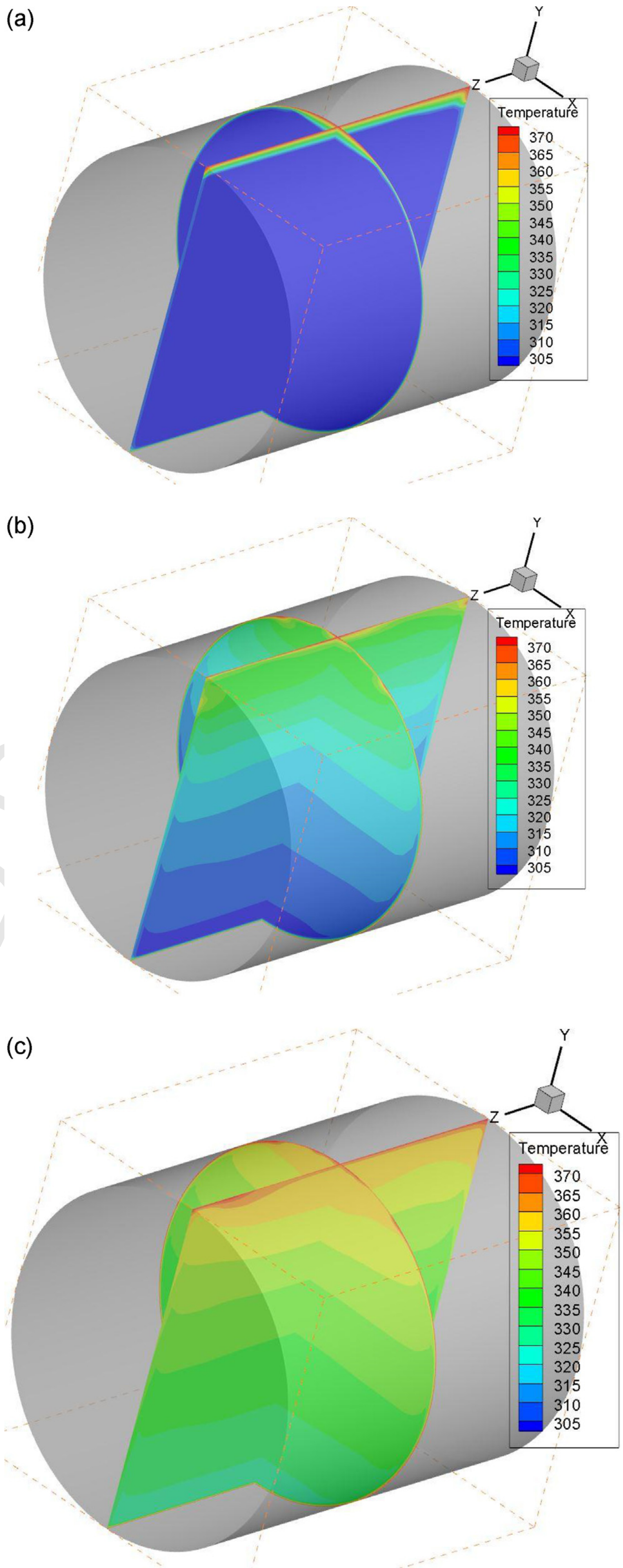

Fig. 9 – Temperature (K) contours in the central *x*- and z-plane of the computational geometry at the (a) beginning (1 s); (b) 30 s; and (c) 90 s of the 20 rpm reciprocal agitation case.

validation and simulations to determine the effect of reciprocal agitation rate.

Following this, the model was validated compared to the experimental data obtained under different reciprocal agitation conditions (summarized in Fig. 2). Fig. 4b shows the comparison of the can centre temperature data with respect to the model results for the first 75 s of the process. As observed in this figure, the model results demonstrated the validity of the developed computational model. Even though the simulation results compared well with the experimental data, there was a difference between the simulation results and experimental data. However, considering the complex nature

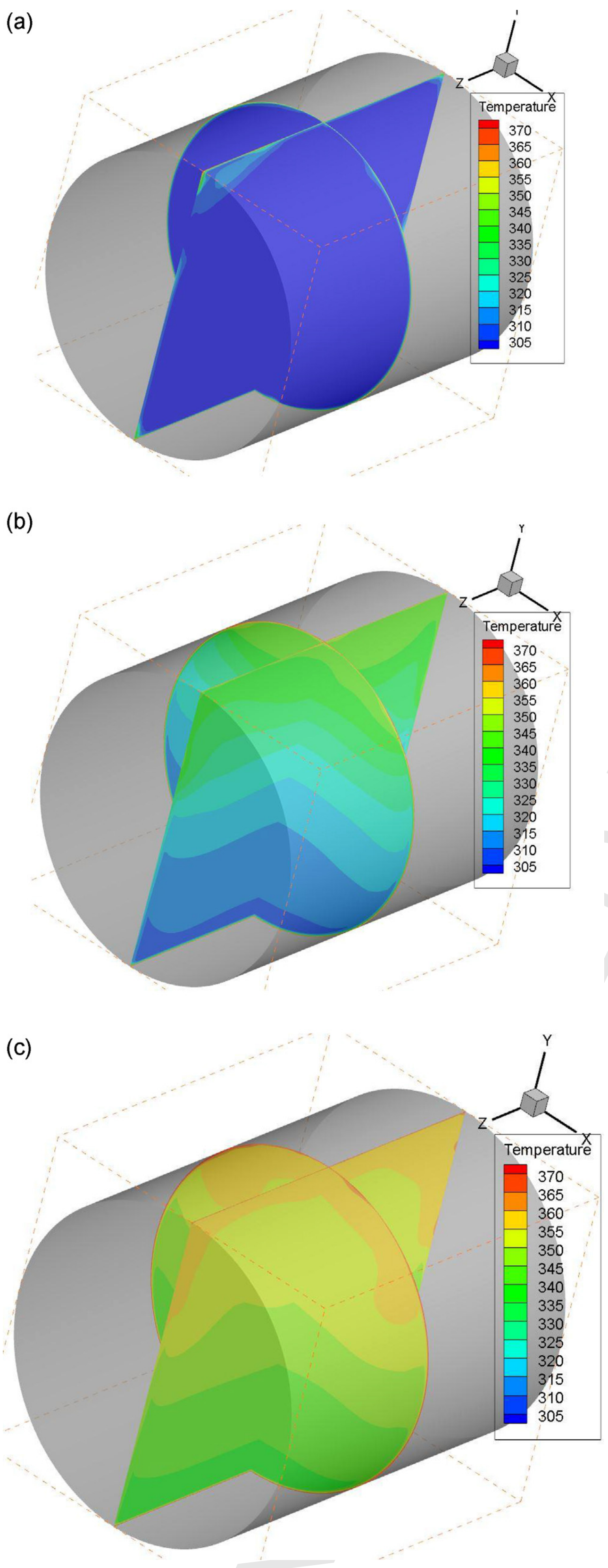

Fig. 10 – Temperature (K) contours with in the central x- and z-plane of the computational geometry at the (a) beginning (1 s); (b) 30 s; and (c) 90 s of the 80 rpm reciprocal agitation case.

of the process and experimental conditions, the model predictions caught the trend of the experimental temperature data. After 75 s of the processing, the model validation case study did not continue to run due to very high requirement of computational time. It took 39.3 h to complete a 1 s of the simulation for validation purpose under 80 rpm reciprocal agitation in an Intel Zeon 4-Core, 3.7 GHz – 32 GB RAM system.

3.2. *Effect of reciprocal agitation rate*

After validating the model, effect of the reciprocal agitation rates from 20 to 140 rpm on the temperature evolution in the cans were tested. Fig. 5 shows the comparison of tangential velocity values for 20, 80 and 140 rpm reciprocal agitation rates versus time while Fig. 6 shows the effect of reciprocal agitation rates on the volume average temperature (T_{avg}) increase of the can for the first 100 s of the process. In these simulations, the boundary temperature was set to be boiling conditions as reported above in the first model validation case. As demonstrated in Fig. 6, the effect of reciprocal agitation rate was noticeable, and the increased agitation rates increased the temperature evolution especially until 80 rpm reciprocal agitation. The effect of further increasing the reciprocal agitation over 80 rpm did not result in any significant difference. This effect of reciprocal agitation until a maximum agitation value might be explained by the balance

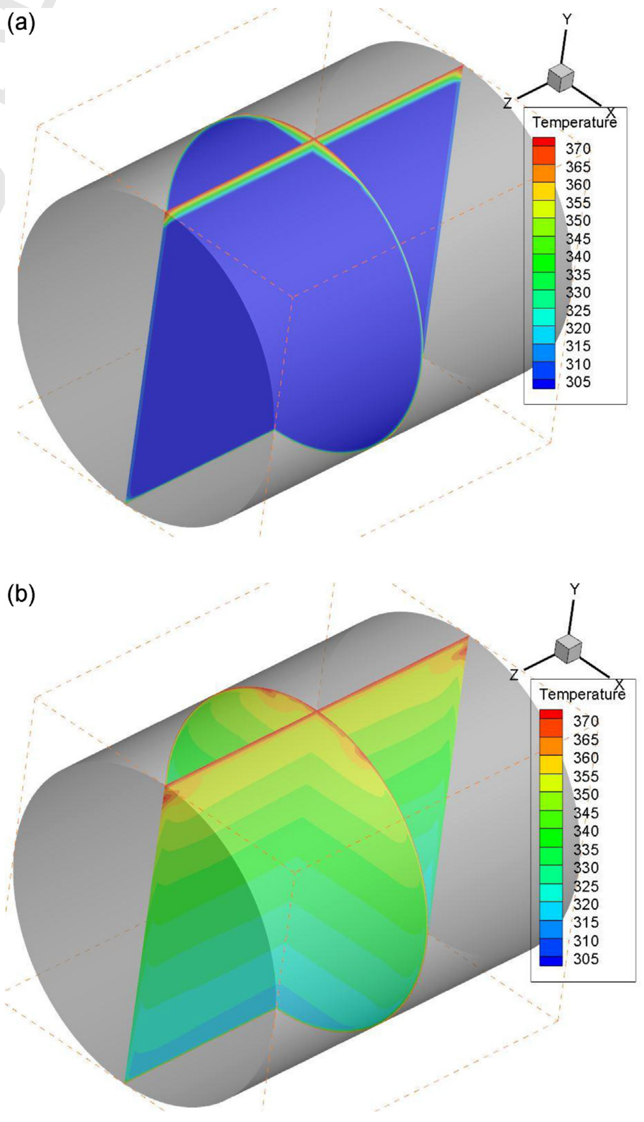

Fig. 11 – Temperature (K) contours in the central x- and z-plane of the computational geometry at the (a) beginning (1 s); (b) 90 s of the 0 rpm (natural convection heating case).

between the agitation, gravitational buoyancy and viscous forces governing the reciprocal agitation process.

As indicated by Boonpongmaee and Makotani (2009) and Tutar and Erdogdu (2012), the flow field during an agitation process involves complex interactions of centrifugal – rotational, gravitational buoyancy and viscous forces. Based on this concept, the following force analysis was performed to better understand the temperature evolution during the reciprocal agitation process as a function of gravitational, agitation and viscous forces:

$$\frac{f_{cbf}}{f_{gbf}} = \frac{\omega^2 r}{g} \tag{15}$$

$$\frac{f_{\text{inertial}}}{f_{\text{viscous}}} = \frac{\omega^2 r^4}{\nu^2} \tag{16}$$

where r was the crank radius of the system (0.075 m), g was the gravitational acceleration (9.81 m/s^2), and ν was kinematic viscosity (m^2/s), f_{cbf}, f_{gbf}, f_{inertial} and f_{viscous} were centrifugal buoyancy, gravitational buoyancy, agitation related forces and viscous forces, respectively, and ω was the dimensional speed of rotation (1/s). ω was shown by ($\omega = 2\pi f/60$) where f was the horizontal agitation rate (rpm). Eqs. (15) and (16) represented Froude and Taylor numbers, respectively.

The ($\omega^2 r$) value, in fact, showed the effect of horizontal agitation rate over the gravitational acceleration, and it was defined to be the reciprocation intensity (g_0):

$$g_0 = \omega^2 \cdot r \cdot \left(1 + \frac{r}{L}\right) \tag{17}$$

where L was the length of the connectivity rod (0.5 m) of the slider crank type system used in the experimental studies. Considering that [$(r/L = 0.15) < 1$], the reciprocation intensity was approximated by:

$$g_0 = \omega^2 \cdot r \tag{18}$$

This was used in the definition of Froude number to demonstrate the reciprocation effect over gravitational force. Froude number increased from 0.03 to 1.64 with the increase of the horizontal agitation rate from 20 to 140 rpm. Simultaneously, Taylor number increased from 2.26E8 to 1.18E10, from 3.65E9 to 2.29E10 and from 1.13E10 to 6.87E10 at the 100 s of 20, 80 and 140 rpm shaking, respectively. The increase ratio of Taylor number was 5.22, 6.27 and 6.08 (these ratios were between the Taylor number values obtained at the 100 and 1 s of the process) for these 3-reciprocal agitation rates. This change in the Taylor number indicated that the reciprocal agitation forces started showing their impact even at low agitation rates, but this effect increased to a certain highest value at 80 rpm. The effect of inertial forces obtained by the horizontal agitation over viscous forces as an internal resistance of the processed liquid was not significant beyond 80 rpm. The further increase after 80 rpm agitation rate did not make any significant effect on the Taylor number increase in the given process, and did not lead to any further temperature increase. In fact, the volume average temperature increase obtained with 80 rpm agitation was over the case of 140 rpm towards the end of the process (Fig. 6) as also indicated by the increase

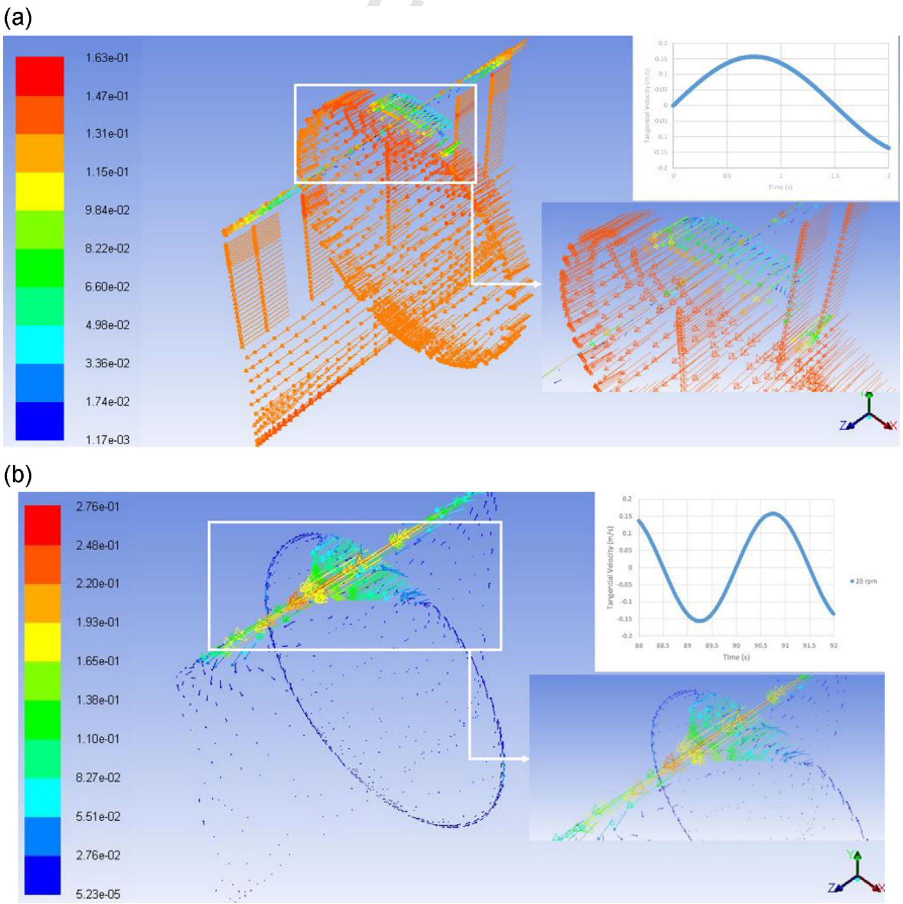

Fig. 12 – Instantaneous velocity vectors (m/s) on x–z and y–z mid-planes of the flow domain at (a) 1 s (very beginning of the agitation) and (b) 90 s (towards the end of the agitation) at 20 rpm.

ratio in Taylor number. Froude number was 0.54 at 80 rpm, and this value was 50% of the gravitational acceleration effect.

As indicated by Walden and Emanuel (2010), the reciprocal agitation apparently used the horizontal acceleration in addition to gravity forces, and the sum of these forces enabled a considerable temperature increase while the further increase after 80 rpm was prevented via the effect of viscous forces. Even though the reciprocation intensity was 1.64 times higher than the regular natural convection case governed by the gravitational acceleration at 140 rpm, the temperature increase did not gain any more benefit from this high rate of agitation. The lower viscosity of the liquid (water) also played a significant role in this concept, and its effect is expected to be more pronounced for the case of non-Newtonian higher viscosity liquids. Trevino (2009) also noted that the oscillating technology with racking movement (reciprocally agitation) might not be beneficial for processing low (1% starch–water mixture) and high (5% starch–water mixture) viscosity products where a comparison of the effects of oscillating and static retort thermal processing was carried out. However, it was also stated that an effective heat transfer rate might be possible to obtain for medium viscosity (3% starch–water mixture) products.

Tutar and Erdogdu (2012) explained that, in agitation related processes, headspace – air bubble moves through via the given effect of agitation and viscosity forces. This leads to the mixing to increase the heat transfer rate. For the case of low viscosity Newtonian liquids, however, this mixing effect is hardly seen, and the air bubble generally might move through the top over the process under a certain effect of agitation rate. Figs. 7 and 8 show the phase (Phase2 – headspace) contours (headspace shown with red contour at the beginning of the process) at the beginning (1 s), 30 and 90 s of the 20 and 80 rpm cases in the various x- and z-planes of the computational geometry, respectively. As observed in Fig. 7, headspace moved at the top of the geometry continuously with the given movement of the can at 20 rpm reciprocal agitation rate. However, the 80 rpm agitation led to an abrupt change of the headspace distribution due to the sudden start of the higher agitation. The considerable difference between 20 and 80 rpm agitation rates was also shown in Fig. 5. Fig. 8a shows the sudden disruption of the headspace at the beginning compared to the case of 20 rpm and a certain inhomogeneous distribution through the process (Figs. 8b, c). At the 90 s of the process, based on the phase contours, it might be assumed that a low amount of headspace was mixed in the water at 20 rpm agitation rate while this was higher at 80 rpm agitation rate. This mixing also brought a considerable and homogeneous temperature increase compared to the case of 20 rpm.

Figs. 9 and 10 show the temperature distribution through the can for 20 and 80 rpm, respectively. The more homogeneous distribution nature of the temperature contours are observed at 80 rpm agitation rate while the 20 rpm agitation rate resembled more like a natural convection case with the distinctly stratified temperature contours. The natural

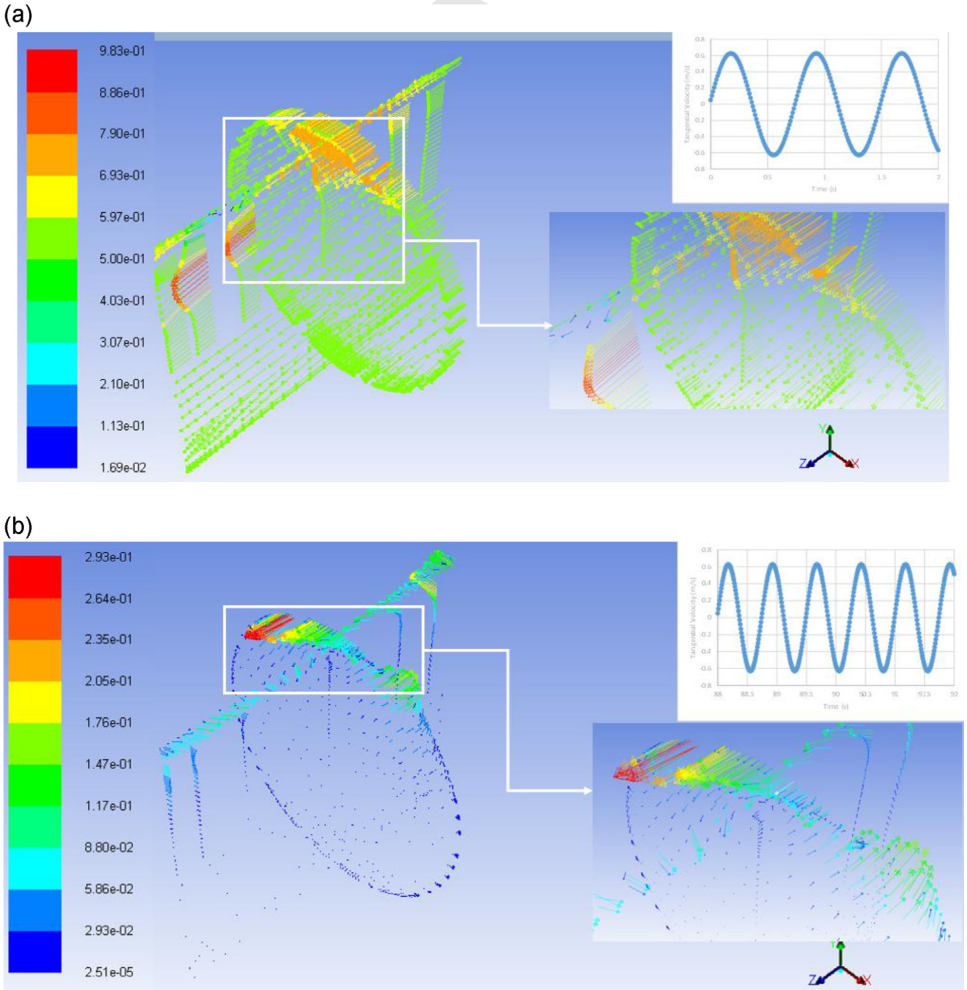

Fig. 13 – Instantaneous velocity vectors (m/s) on x–z and y–z mid-planes of the flow domain at (a) 1 s (very beginning of the agitation) and (b) 90 s (towards the end of the agitation) at 80 rpm.

Please cite this article in press as: Erdogdu, F., et al., Determining the optimal shaking rate of a reciprocal agitation sterilization system for liquid foods: A computational approach with experimental validation. Food Bioprod Process (2016), http://dx.doi.org/10.1016/j.fbp.2016.07.012

convection case was summarized in Fig. 11. Figs. 12 and 13, on the other hand, comparatively represented the instantaneous velocity vectors obtained on the xz and yz mid-planes of the flow domain at 1 (very beginning of the agitation motion) and 90 s (towards the end of the agitation motion) at 20 and 80 rpm, respectively to further compare the agitation effects for the field of flow motion. When the agitation started, the headspace was immediately affected, and it could not maintain its shape and orientation with respect to the water flow domain, which was accelerated like a solid body motion due to the horizontal acceleration as seen in Figs. 12a and 13a. As the agitation motion continued, dynamic pressure developed in the flow domain, and different spatial and temporal evolution of the fluid flow, depending upon the simulation time and agitation rate, were clearly identified from the instantaneous velocity vectors in the vicinity of the air–water interface whose shape and position became highly unstable with the increasing agitation rate (Figs. 12b and 13b). Superposition of inertial, agitation and natural forces due to gravitational forces (mixing convective forces) became more evident and effective on the air–water flow domain at higher agitation rate of 80 rpm, leading to higher inertial and convective instabilities of the present two-phase flow system with more complex, three-dimensional flow behaviour in the whole domain system. This behaviour eventually would make a positive effect on the temperature evolution for 80 rpm compared to 20 rpm as previously observed in the temperature contours in Fig. 10. With this positive effect, forced convective heat transfer mechanism on the temperature evolution became more dominant as the agitation rate increased up to 80 rpm and did not change at higher agitation rates as also explained above.

4. Conclusions

This study introduced determining the optimal reciprocal agitation rate based on the experimentally validated computational model. The computational model was used to determine the temperature change in a can filled with water with 2% headspace undergoing a reciprocal agitation process, and the temperature evolution during the process was determined to be under control of reciprocation intensity and the ratio of agitation and viscous forces. The computational results indicated a certain limit of reciprocal agitation rate in the view of temperature increase indicating the significant effect of viscosity and inertial forces obtained by the agitation. For a Newtonian low viscosity liquid case, represented by water, the 80 rpm reciprocal agitation rate was determined to be an optimum rate.

It would be valuable to determine the optimum agitation conditions for high viscosity non-Newtonian liquids considering that a significant portion of the food products processed in cans lie in this category. Besides, a further study to demonstrate the effect of headspace volume to increase the agitation rates for liquid and particulate food products would also be required.

Acknowledgement

This study was developed within the framework of the ERA-net SUSFOOD Sunniva project, “Sustainable food production through quality optimized raw material production and processing technologies for premium quality vegetable products and generated by-products”. The following acknowledgements are recognized by the authors:

Ferruh Erdogdu acknowledges the Ministry of Food, Agriculture and Livestock (GDAR) of Turkey for the travel support to attend the project meetings.

Mustafa Tutar acknowledges the support from the Daniel and Nina Carasso Foundation, France Q3 (www.fondationcarasso.org) and the Department of Economic Development and Competitiveness (ELIKA).

Sigurd Oines and Dagbjorn Skipnes acknowledge the support from the Research Council of Norway through grant no. NO 10829.

References

Ates, M.B., Skipnes, D., Rode, T.M., Lekang, O-I., 2014. Comparison of bacterial inactivation with novel agitating retort and static retort after mild treatments. Food Control 43, 150–154.

Bermudez-Aguirre, D., Lima, F., Reitzel, J., Garcia-Prez, M., Barbosa-Canovas, G.V., 2013a. Evaluation of total heat transfer coefficient (hT) during innovative retort processing: static, gentle motion and rocking mode. In: IFT Annual Meeting, Abstract number: 031-02.

Bermudez-Aguirre, D., Lima, F., Reitzel, J., Garcia-Prez, M., Barbosa-Canovas, G.V., 2013b. Development of a mathematical model to describe heat transfer using three different processing modes. In: IFT Annual Meeting, Abstract Number: 031-138.

Boonpongmaee, T., Makotani, Y., 2009. Heat transfer in rotating cylindrical cells with partitions. Int. J. Heat Fluid Flow 30, 211–217.

Clifcorn, I.E., Peterson, G.T., Boyd J. m. O'Neil, J.H., 1950. A new principle for agitating in processed canned foods. Food Technol. 4, 450–460.

Erdogdu, F., Tutar, M., 2012. A computational study for axial rotation effects on heat transfer in rotating cans containing liquid water, semi-fluid system and headspace. Int. J. Heat Mass Transf. 55, 3774–3788.

Hirt, C.W., Nichols, B.D., 1981. A computational method for pressure 0 surface hydrodynamics. J. Press. Vessel Technol. – Trans. ASME 103, 136–141.

Julien, K., Legg, S., McWilliams, J., Werne, J., 1996. Hard turbulence in rotation Rayleigh-Benard convection. Phys. Rev. E 53, R5557.

Kooij, G.L., Botchev, M.A., Geurts, B.J., 2015. Direct numerical simulation of Nusselt number scaling in rotating Rayligh-Benard convection. Int. J. Heat Fluid Flow 55, 26–33.

Liffman, K., Metcalfe, G., Cleary, P., 1997. Convection due to horizontal shaking. In: CSIRO-1997: International Conference on CFD in Mineral and Metal Processing and Power Generation, pp. 165–168.

Ohlsson, T., 1980. Optimal sterilization temperatures for sensory quality in cylindrical containers. J. Food Sci. 45, 1517–1521.

Pesch, W., Palaniappan, D., Tao, J., Busse, F.H., 2008. Convection in heated fluid layers subjected to time-periodic horizontal accelerations. J. Fluid Mech. 596, 313–332.

Reader, G.T., Hooper, L.C., 1982. Stirling Engines. Spon Press, Oxfordshire, UK.

Rosnes, J.T., Skara, T., Skipnes, D., 2011. Recent advances in minimal heat processing of fish: effects on microbial activity and safety. Food Bioprocess Technol. 4, 833–848.

Singh, A.P., Singh, A., Ramaswamy, H.S., 2015a. Modification of a static steam retort for evaluation heat transfer under reciprocation agitation thermal processing. J. Food Eng. 153, 63–72.

Singh, A., Singh, A.P., Ramaswamy, H.S., 2015b. A refined methodology for evaluation of heat transfer coefficients in canned particulate fluids under rapid heating conditions. Food Bioprod. Process. 94, 169–179.

Singh, A., Ramaswamy, H.S., 2015a. Effect of product-related parameters on heat-transfer rates to canned particulate non-Newtonian fluids (CMC) during reciprocating agitation thermal processing. J. Food Eng. 165, 1–12.

Singh, A.P., Ramaswamy, H.S., 2015b. Effect of Can orientation on heat transfer coefficients associated with liquid particulate mixtures during reciprocation agitation thermal processing. Food Bioprocess Technol. 8, 1405–1418.

Singh, A., Singh, A.P., Ramaswamy, H.S., 2016. A controlled agitation process for improving quality of canned green beans during agitation thermal processing. J. Food Sci. (in press).

Singh, A.P., Ramaswamy, H.S., 2016. Simultaneous optimization of heat transfer and reciprocation intensity for thermal processing of liquid particulate mixtures undergoing reciprocating agitation. Innov. Food Sci. Emerg. Technol. 33, 405–415.

Trevino, J., (master of science thesis) 2009. Effect of Oscillating and Static Retort Thermal Processing Technology Using and Institutional Size Pouch. Clemson University, Clemson, SC, USA.

Tutar, M., Erdogdu, F., 2012. Numerical simulation for heat transfer and velocity field characteristics of two-phase flow systems in axially rotating horizontal cans. J. Food Eng. 111, 366–385.

Ubbink, O., Issaa, R.J., 1999. A method for capturing sharp fluid interfaces on arbitrary meshes. J. Comput. Phys. 153, 26–50.

Walden, R., Emanuel, J., 2010. Developments in in-container retort technology: the Zinetec Shaka process. In: Doona, C.J., Kustin, K., Feery, F.E. (Eds.), Case Studies in Novel Food Processing Technologies: Innovation in Processing, Packaging and Predictive Modelling. Woodhead Publishing Ltd., Cambridge, UK.

Yakhot, H.Q., Orszag, S.A., 1986. Renormalization group analysis of turbulence. I. Basic theory. J. Sci. Comput. 1, 1–51.